Apparent non-statistical binding in a ditopic receptor for guanosine.

Asawin Likhitsup,[†] Robert J Deeth,[†] Sijbren Otto,[‡] Andrew Marsh[†]*

[†]*Department of Chemistry, University of Warwick, Coventry, CV4 7AL, United Kingdom.*

a.marsh@warwick.ac.uk

[‡]*Department of Chemistry, University of Cambridge, Lensfield Road, Cambridge, CB2 1EW, United Kingdom.*

<Graphical abstract>

Introduction

Quantitation of the interaction of guest molecules with receptors bearing multiple binding sites is of significance across supramolecular chemistry, structural biology, pharmacology of biological receptors and materials science.[1] Elucidating mechanistic pathways of association,[2-5] including whether or not they take place with what is referred to as 'cooperativity',[6-8] is thus of practical importance. We report here the binding studies of ditopic receptors for guanosine and the observation of what appears as a non-statistical,[9] or cooperative binding event. The C_2-symmetric ditopic receptors are composed of two cytidine moieties[10] linked through either an alkyne, **1** or dialkyne, **2** at C5 (**Figure 1**) as reported previously.[11] Job's plot revealed a 1:2 stoichiometry of binding between **1** or **2** with **3** and the association constants were reported in deuterochloroform as 2670 and 2200 M^{-2}, respectively, using a naïve 1:2 binding model. We move herein towards a more complete analysis of the equilibria involved, whilst recognising the limitations of the methods employed. Receptors with more than one mode of association

present real challenges in terms of experimental design, data acquisition and the mathematical algorithms required to unambiguously assign association constants, particularly of relatively weakly interacting supramolecular assemblies.[12, 13]

<Figure 1>

Curve fitting methods

NMR titration is an accessible and informative method used in determining association constants between both small and large molecules in solution.[14-17] Titration data may be analysed by: (i) graphical methods such as the Benesi-Hildebrand (double reciprocal) plot and Scatchard plot; or (ii) direct curve fitting methods. Curve fitting methods require no approximations and allow almost unrestricted distribution of experimental points (host and guest concentrations), within usual limitations.[17, 18] For example, the Saunders-Hyne method[19] (two-state approximation) has been used to determine the strength of hydrogen bonded aggregates.[20] A number of computer programs have been created for curve fitting; however, those more commonly available are limited to 1:1, 1:2 or 2:1 complexes.[15] Several commercial programs (including Specfit/32™ [21] HypNMR[22] Dynafit[23] and Prism[24]) and non-commercial algorithms (EQNMR,[25, 26] NMRTit,[27] HOSTEST,[28] and ASSOCIATE as recently implemented[29]) allow more sophisticated models to be used, although each has limitations. In more complex cases, numerical methods are the best solution because of the number of parameters involved. Recently, a complete treatment that allows complex two component systems of the type studied herein to be tackled has been disclosed, and its eventual application to this system will no doubt be revealing.[13]

In the case of 1:1 complexes, curve fitting is usually straightforward.[30] When a 1:2, 2:1 complex, or multiple equilibria are present, finding the mathematical solution for curve fitting becomes progressively more problematic and some results using this approach have been found to be less satisfactory by some authors.[31-33] In the case of weak 1:2 complexes with $K_1 << K_2$, it has been shown that the determination of the stepwise binding constants is not possible.[31]

Results and discussion

Self-association of receptors 1 and 2

Previous studies on a lipophilic cytidine derivative have revealed weak self-association with a dimerisation constant of 30-40 M^{-1},[34, 35] also observed in a portion of the crystal structure of **2** (**Figure 2**).[11] Thus, we set out to re-evaluate the self-association of **1** and **2** using ^{1}H-NMR dilution[14] in the first instance. Expecting a relatively weak association constant, we chose an initial concentration of about 0.01 M in deuterochloroform, meeting usual criteria for its accurate determination,[16, 17] *i.e.* that $\frac{1}{10} \bullet \frac{1}{K_a} \le [G]_t \le 10 \bullet \frac{1}{K_a}$ w here K_a is the expected association constant and $[G]_t$ is the total concentration of guest to be diluted.

<Figure 2>

The ^{1}H-NMR spectra of **1** and **2** in deuterochloroform are very similar, but in **1** H-6 appears at 8.14 ppm, whilst for **2** H-6 appears at 8.22 ppm. The two exocyclic NH_2 protons are non-equivalent with NH^a appearing at higher field than H^b: 5.6-5.9 and 5.6-6.0 ppm for **1** and **2** respectively, in agreement with previous observations.[34]

The dimerisation of **2** was initially studied by monitoring the NMR chemical shifts of NH^a, NH^b and H-6 upon dilution (tabulated in **Supporting Information Part 2**). Except for the first data point the concentration of the receptor was calculated using tetramethylsilane as an internal standard. This complete data set was fitted using the Saunders-Hyne model,[14, 15] assuming that only two major components (monomer and dimer) are significant in the equilibrium,[19] resulting in the curves shown in **Figure 3** giving the host dimerisation constant, $K_{\mathbf{2}\bullet\mathbf{2}}$ as 340±7 M^{-1} in deuterochloroform. Errors were estimated by adapting a least-squares method[36, 37] whereby data points in the spreadsheet are sequentially deleted and a new least-squares fit carried out to estimate the association constant lacking that data point. The complete data set could not be fitted at all to either a trimer model (data not shown), or a 'dimer of dimers' model *(c.f.* self-association of guanosine **3**). Further confidence in the quality of the dataset and fitting comes from evaluation of the probability of binding,[17] $p = 2 \times \frac{[2 \bullet 2]}{[2]_{tot}}$), found to be 0.37 < $p_{\mathbf{2}}(\mathbf{2}\bullet\mathbf{2})$ < 0.82 over the titration interval (see **Supporting Information part 2**). The best quality data and fitting is found for 0.20 < p < 0.80, although data outside this range is most useful if errors therein can be fully described.

<Figure 3>

One limitation of the model used is that it cannot distinguish dimerisation from isodesmic polymeric association.[12, 38] In order to do this, an independent method such as VPO,[12] other methods for estimating M_n or M_w, or more sophisticated numerical approaches[13] are required. The same dilution process was also studied by isothermal

titration calorimetry (ITC; see Supporting Information Part 1) and fitted using a dimerisation model to give an association constant $K_{\mathbf{2}\bullet\mathbf{2}}$ = 90 M^{-1}.which is noticeably different, although much closer to $K_{\mathbf{1}\bullet\mathbf{1}}$ observed for the shorter receptor **1**.

Minor conformational change of **2** upon dimerisation results in shielding of H-6 and deshielding of NH^a. Upon dilution, the signal for H-6 shifted downfield ($\Delta\delta$ = 0.08 ppm) whilst that for NH^a moved upfield ($\Delta\delta$ = 0.37 ppm). The effect of the alkyne is more pronounced in NH^a due to greater proximity of the alkyne π-orbital compared to H-6. Although the NMR titration result agrees with the dimerisation model, receptor **2** may also form a hydrogen bonded tape at higher concentration, observed as a viscous gel in chloroform, leading ultimately to the solid state structure reported previously.[11] The only significant difference in the ^{1}H-NMR spectra of **1** and **2** is that H-6 of **1** appears at higher field. Upon dilution, all three protons are shifted in the same way as in **2**: H-6 downfield, NH^a upfield and NH^b upfield (**Figure 4**). Again, conformational changes may be used to explain the peak shifts of H-6 and NH^a.

Treatment of the NMR shift data from the dilution of monoalkyne **1** by simultaneous curve fitting of H-6, NH^a and NH^b revealed $K_{\mathbf{1}\bullet\mathbf{1}}$ = 83±3 M^{-1} in deuterochloroform. The probability of binding for the receptor **1** in the dimer, p_1(**1**•**1**) was found to be $0.18 < p_1(\mathbf{1}\bullet\mathbf{1}) < 0.67$ over the titration interval. The association constants for lipophilic cytidines have been consistently reported to be around 30-40 M^{-1}.[35, 41] Since there are two cytidines in each receptor, the dimerisation constant of 83±3 M^{-1} for **1** is consistent with the reported values, although it contrasts with the higher value of 340±7 M^{-1} found for dialkyne **2**.

<Figure 4>

Self-association of guanosine derivative 3

The structure of lipophilic guanosine in chloroform has been extensively studied by Gottarelli and co-workers.[42-44] It has been shown that **3** readily dimerises through hydrogen bonding between N3-H and O4 (**Figure 5**). At high concentration, the weaker hydrogen bonds between N1 and N2-H connect the dimers together to form guanosine ribbons (in the absence of metal ions) resulting in the observation of viscous gels.[44]

<Figure 5>

In order to devise a model for curve fitting, the following equilibria are considered:

$$\mathbf{3} + \mathbf{3} \overset{K_{\mathbf{3}\cdot\mathbf{3}}}{\rightleftharpoons} \mathbf{3}\bullet\mathbf{3}$$

$$\mathbf{3}\cdot\mathbf{3} + \mathbf{3}\cdot\mathbf{3} \overset{K_{\mathbf{3}\cdot\mathbf{3}\cdot\mathbf{3}\cdot\mathbf{3}}}{\rightleftharpoons} \mathbf{3}\cdot\mathbf{3}\cdot\mathbf{3}\cdot\mathbf{3}$$

$$K_{\mathbf{3}\cdot\mathbf{3}} = \frac{[\mathbf{3}\cdot\mathbf{3}]}{\mathbf{3}^2} \quad (1)$$

$$K_{\mathbf{3}\cdot\mathbf{3}\cdot\mathbf{3}\cdot\mathbf{3}} = \frac{[\mathbf{3}\cdot\mathbf{3}\cdot\mathbf{3}\cdot\mathbf{3}]}{\mathbf{3}^4} \quad (2)$$

Mass balance: $$[\mathbf{3}]_0 = [\mathbf{3}] + 2\times[\mathbf{3}\cdot\mathbf{3}] + 4\times[\mathbf{3}\cdot\mathbf{3}\cdot\mathbf{3}\cdot\mathbf{3}] \quad (3)$$

Chemical shift: $$\delta_{cal} = \chi_{\mathbf{3}}\delta_{\mathbf{3}} + \chi_{\mathbf{3}\cdot\mathbf{3}}\delta_{\mathbf{3}\cdot\mathbf{3}} + \chi_{\mathbf{3}\cdot\mathbf{3}\cdot\mathbf{3}\cdot\mathbf{3}}\delta_{\mathbf{3}\cdot\mathbf{3}\cdot\mathbf{3}\cdot\mathbf{3}} \quad (4)$$

Rearrangement and substitution of (1) and (2) into (3) gives a polynomial equation. If curve-fitting is performed using the solution of this equation, problems arise in selecting the correct non-imaginary root.[45] This method is inflexible and time-consuming because the mathematical solution for the polynomial must be derived for

each system. It is therefore not surprising that most curve-fitting programs only extend to 1:2 binding.[15 16, 46]

In order to address this problem, a more flexible curve-fitting routine was devised based on NMR chemical shift simulation using numerical methods in MS Excel®.[36] The method, as described by Wilcox and co-workers, has been employed in the study of ternary systems.[47] This routine requires an input of $K_{\mathbf{3}\bullet\mathbf{3}}$ and $K_{\mathbf{3}\bullet\mathbf{3}\bullet\mathbf{3}\bullet\mathbf{3}}$, with a known initial concentration $[\mathbf{3}]_0$; there is only one set of [**3**], [**3•3**], and [**3•3•3•3**] that satisfies equations (1), (2) and (3).

Using this template, the 'Solver' function in Microsoft Excel® was used to find the value of [**3**] at each concentration with the input K values (see **Experimental** for details). We then calculated δ_{cal} from the input $\delta_{\mathbf{3}}$, $\delta_{\mathbf{3}\bullet\mathbf{3}}$ and $\delta_{\mathbf{3}\bullet\mathbf{3}\bullet\mathbf{3}\bullet\mathbf{3}}$, parameters that were readily easily estimated from the titration curve. Non-linear least squares curve fitting was then performed by varying $\delta_{\mathbf{3}}$, $\delta_{\mathbf{3}\bullet\mathbf{3}}$ and $\delta_{\mathbf{3}\bullet\mathbf{3}\bullet\mathbf{3}\bullet\mathbf{3}}$ to give the best fit between δ_{cal} and δ_{obs}. The association constants $K_{\mathbf{3}\bullet\mathbf{3}}$ and $K_{\mathbf{3}\bullet\mathbf{3}\bullet\mathbf{3}\bullet\mathbf{3}}$ were iterated manually and the pair that gave the smallest sum of chi squared (S) values from curve fitting was chosen. Errors were again estimated by the same adapted least-squares method as previously.[36, 37] The algorithm was benchmarked against recent literature data[48] where the challenge of 2:1 binding was faced using a modified commercial HypNMR package,[26] underlining the non-standard nature of the task (see **Supporting Information Part 1**). The new spreadsheet was able to replicate the observed equilibrium constants in that 2:1 system satisfactorily.

The NMR spectrum of **3** shows only two sets of amine signals. Unlike the NH_2 in cytidine, the guanosine NH_2 rotates quickly on the NMR timescale and the two exocyclic

NHs are magnetically equivalent.[34] Upon dilution, the N3-H shifts downfield from 11.99 to 12.08 ppm. Similarly, H-8 shifts downfield from 7.76 to 7.81 ppm. Analogously, NH_2 shifts upfield from 6.25 to 5.90 ppm (**Figure 6**). Since the induced chemical shifts for H-8 and NH_2 are relatively small, curve fitting based on these shifts alone might give rise to a higher systematic error than the current procedure, fitting all the limiting chemical shifts for H-8, NH_2 and N3-H in a single step to minimize the combined *S* values. The two association constants were then carefully iterated to find the best solutions, with an error limit representing the standard deviation of least-squares fits lacking sequential data points as above. The resulting association constants in deuterochloroform, $K_{\mathbf{3\bullet3}}$ and $K_{\mathbf{3\bullet3\bullet3\bullet3}}$ are found to be 370±72 and 15±1 M^{-1} respectively, in agreement with a previous report (K_{dimer} 300 M^{-1}), although higher order aggregates were not recognised that analysis.[35] The probability of binding for significant aggregated species over the titration interval was found to be $0.53 < p_G(\mathbf{G\bullet G}) < 0.66$ and $0.015 < p_G(\mathbf{G_2\bullet G_2}) < 0.31$ respectively.

Preliminary ITC results are inconclusive since the data could not be fitted properly to a calculated curve using the above 'dimer of dimers' model, although this may be due to way data is treated following standard ITC experiments (see **Supporting Information Part 1**).

<Figure 6>

Binding studies of receptors 1 and 2 with guest 3

Binding studies between receptors **2** and **3** (**Figure 7**) were carried out by NMR titration in $CDCl_3$. The input for the freely available NMRTit program[27] requires that concentration of the host **2** is held constant throughout the experiment. In the first attempt, the titrant **3** was dissolved with host **2** stock solution, as required, but the concentration of **2** was now so low that it was impossible to unambiguously follow the now broad N-H signals (chosen since they presented the greatest change in chemical shift) in the ^{1}H-NMR spectrum. Thus, the titration was performed by adding a concentrated solution of **3** in small portions to a relatively concentrated solution (*ca.* 0.01 M) of **2** in the NMR tube, thereby allowing concentration of host **2** to change with each addition of guanosine **3**. It was recognised that data analysis would no longer be possible using, for example NMRTit, but one benefit is that binding of receptor to guest stays within the preferred 20-80% even when a 3-fold excess of guest has been added. This would be more difficult to achieve whilst maintaining practicable dynamic range in the NMR experiment if more host were added together with guest in order to maintain constant host concentration. The NH^b in **2** was followed as it is directly involved in hydrogen bonding to the guest and the induced chemical shift change is quite large. The initial data point now overlapped with that for the experiment to determine host dimerization, [*HG*] = 0 (see **Supporting Information Part 2**), adding confidence to the data fitting. All concentration changes were calibrated using the aromatic peak areas (H-6 for **2** and H-8 for **3**) against TMS as an internal standard.

<Figure 7>

The equilibria considered are shown in **Scheme 1** (*H* = host, *G* = guest).

<Scheme 1>

And following the standard Saunders-Hyne model,

Association constants: $$K_{HG} = \frac{[HG]}{[H][G]} \quad (5)$$

$$K_{HGG} = \frac{[HGG]}{[H][HG]} \quad (6)$$

Mass balance for both host and guest is

$$[H]_0 = [H] + 2[HH] + [HG] + [HGG] \quad (7)$$

$$[G]_0 = [G] + 2[GG] + 4[G4] + [HG] + 2[HGG] \quad (8)$$

The chemical shift was calculated from the contribution of all the species present in the equilibrium according to Scheme 1:

$$\delta_{cal} = \chi_H \delta_H + \chi_{HH} \delta_{HH} + \chi_{HG} \delta_{HG} + \chi_{HGG} \delta_{HGG} \quad (9)$$

The limiting chemical shift of host dimer **2•2** as well as the self-association constants for both **2** and **3** were taken from NMR dilution studies described above. Upon addition of guest **3**, NH^b of **2** shifted downfield from 7.2 to 9.8 ppm. From the curve fitting (**Figure 8**), the stepwise association constants are found as $K_{\mathbf{2•3}}$ = 8100 ± 380, $K_{\mathbf{3•2•3}}$ = 1170 ± 80 M^{-1} in deuterochloroform. Hence the overall microscopic association constant $K_a = K_{HG}K_{HGG}$ from NMR titration is 9.56×10^6 M^{-2}. The probability of binding of **3** in forming the termolecular complex is described by 0.10 < $p_{\mathbf{3}}$ (**3•2•3**) < 0.60 over the titration interval. A speciation curve for **2** upon addition of **3** is shown in **Figure 9** and

corresponding graphical probability of binding data is given in **Supporting Information Part 2**.

<Figure 8>

<Figure 9>

The NMR titration between **1** and **3** and subsequent curve fitting was performed by the same method (**Figure 10**) whereby stepwise association constants were found to be $K_{\mathbf{1\bullet3}}$ = 5180 ± 210 and $K_{\mathbf{3\bullet1\bullet3}}$ = 4800± 170 M^{-1} in deuterochloroform. Hence the overall microscopic association constant $K_a = K_{HG}K_{HGG}$ from NMR titration is 24.86×10^6 M^{-2}. The probability of binding of **3** in forming the termolecular complex is described by $0.14 < p_{\mathbf{3}}(\mathbf{3\bullet1\bullet3}) < 0.77$ over the titration interval. A speciation curve for **1** upon addition of **3** is shown in **Figure 11** and graphical fraction of guest in bound complex (probability of binding) data is presented in **Supporting Information Part 2** .

<Figure 10>

<Figure 11>

Previous studies on the G•C base pair in chloroform solution have revealed consistent association constants of $1.6\text{-}1.7\times10^4$ M^{-1}.[41] Other systems containing DDA•AAD hydrogen bonding complexes show association constants *ca.* 1×10^4 M^{-1}.[49] The stepwise binding constants found here by NMR between **1** and **2** with **3** are somewhat less than these values.

The stepwise binding of receptors **1** and **2** with **3**, summarised in **Figures 12** and **13**) respectively, differs significantly. According to Ercolani's assessment of cooperativity,[6] the ratio between K_{HG} and K_{HGG} should be 4:1 for statistical, or non-cooperative interaction. Binding of just one equivalent of guest **3** to either C_2-symmetric **1** or **2** is a symmetry breaking process, with an expected entropic cost. The second equivalent of **3** then has choice between binding to a new ditopic receptor molecule or the 1:1 complex, giving an apparent stepwise association complex.

<Figure 12>

<Figure 13>

Binding between **2** and **3** gave K_{HG}/K_{HGG} of *ca.* 7:1, suggestive of close to independent, or possibly anti-cooperative, binding, that would be consistent with the statistically expected value (*ca*. 4:1). On the other hand, binding between **1** and **3** gave a K_{HG}/K_{HGG} ratio close to 1, indicating that binding of the first ligand **3** is in some way beneficial to a subsequent binding event, *i.e.* positive cooperativity is observed. The origin of this differing cooperativity must ultimately stem from the different structures of the receptors themselves. We observe from preliminary DFT calculations on simplified analogues of **1** and **2** lacking the ribose rings that rotation around the central alkyne bond alone has no significant energetic cost (data not shown). However, simple molecular model building of mono-alkyne host **1** using the Merck Molecular Mechanics Force Field (MMFF94x, well parameterised for dispersive interactions) with an implicit solvation model,[50] dielectric = 10 indicates that the four bulky triisopropylsilane protecting groups interact to a significant extent (**Figure 14**), translating a rotational motion around the

alkyne axis into a perpendicular geared, or propeller motion. Thus considering the dihedral between *ca*. 200-315° as an energetically neutral position (**Figure 15**) a barrier of *ca.* 2 kcal mol^{-1} is observed at 165°, with a local minimum at 180° and a global minimum between 0-30°. At this point the ribose moieties and bulky TIPS groups are about as far apart as possible. In comparison, close to 165° the two amine groups bypass one another with an overall 'gearing' effect as the TIPS groups also move past each other requiring interacting solvent rearrangement and possibly bringing enthalpic benefit due to dispersive forces once the steric barrier is overcome.

<Figure 14>

<Figure 15>

By contrast, rotation around the same dihedral in dialkyne receptor **2** shows an energy profile consistent with less repulsive interaction between the bulky TIPS groups with only 3 kcal mol^{-1} difference between E_{max} and E_{min}, compared to an overall energy difference of 5.5 kcal mol^{-1} for receptor 1 (**Figure 16**). Whilst this data does not include the presence of a guanosine guest **3**, inspection of models such as **Figure 14** suggests that its presence would reinforce the observed intra-receptor interaction through a combination of steric effects and dispersive interactions. In the case of the longer receptor **2** this pathway is not accessible since the bulky groups are beyond interacting distance. This intra-receptor reinforcement has been observed previously to be a key factor in other host-guest systems that have been demonstrated to display cooperative,[1] or non-statistical binding behaviour.[14, 51, 52] In other words, as demonstrated by speciation curves in **Figures 9** and **11**, the shorter receptor **1** shows an unexpectedly large stepwise

association constant for the binding of a second guanosine molecule, leading to a greater concentration of **1•3•3** than would otherwise be expected.

<Figure 16>

The assignment of such non-statistical behaviour to a binding event is not straightforward, since classic Scatchard plots ought to be applied only to strictly intermolecular binding events.[53] The system presented here meets this criterion and hence in the case of **1•3** can be described as having reinforced,[51] or non-statistical binding, more usually described as exhibiting 'positive cooperativity'. Although such cooperativity has long been recognised in proteins[54] and macromolecules,[55, 56] self-assembly processes involving small molecules, often referred to as 'cooperative', frequently show expected statistical behaviour upon closer analysis. In contrast, the **1•3** pairing investigated here does appear to show non-statistical behaviour. Computational data analysis to further explore these effects in these model systems is ongoing, together with fuller isothermal titration calorimetry data acquisition and interpretation.

Conclusion

The binding of receptors **1** and **2** with **3** has been studied by NMR titration and an improved curve fitting procedure used to analyze the titration result. Compared to the implementation of several algorithms, a number of advantages are apparent, although the limitations of this classic approach as implemented are also becoming clearer.[13] The approach herein allows the use of readily available software to treat more complex systems without use of polynomial equations; additionally by allowing the concentration

of host to vary over the titration interval the fraction of guest bound in the complex, p, remains with the desired range $0.2 < p < 0.8$ over a wider concentration of guest than would be otherwise possible. There remain however issues to be addressed in that: (i) simultaneous fitting of higher equilibria to experimental data presents a more serious programming challenge, especially if errors are to be estimated during that process; (ii) the current approach requires user intervention during the iterations to achieve the best data fit.

The dimerisation constants of **1** and **2** were found to be 83±3 M^{-1} and 340±7 M^{-1} in deuterochloroform respectively. The self-association of guanosine **3** was described in terms of equilibria between monomer, dimer and tetramer and the association constants were found to be $K_{\mathbf{3}\bullet\mathbf{3}}$ 370±72 and $K_{\mathbf{3}\bullet\mathbf{3}\bullet\mathbf{3}\bullet\mathbf{3}}$ 15±1 M^{-1} in deuterochloroform All these self-associations were included in the subsequent curve fitting of the NMR titration data of **1** or **2** with **3** although the limitations of the current approach mean that concurrent optimisation of all equilibria is not yet possible. The stepwise association constants for **1** and **3** were found to be $K_{\mathbf{1}\bullet\mathbf{3}}$ 5180 ± 210 and $K_{\mathbf{1}\bullet\mathbf{3}\bullet\mathbf{3}}$ 4800± 170 M^{-1}, demonstrating non-statistical binding (positive cooperativity). Analogously for **2** stepwise equilibria were $K_{\mathbf{2}\bullet\mathbf{3}}$ = 8100 ± 380, $K_{\mathbf{2}\bullet\mathbf{3}\bullet\mathbf{3}}$ = 1170 ± 80 M^{-1} respectively, which is within the range expected for statistical (non-cooperative) binding. Basic molecular mechanics modelling shows that the mono-alkyne receptor **1** possesses hindered rotation around the central axis that may partly explain the origin of the observed non-statistical binding or positive cooperativity upon interacting with guest **3**. This is notable since there are relatively few examples of small molecule systems that are now understood to display such behaviour.

Experimental

NMR titrations were carried out in $CDCl_3$ (Aldrich) used as received and residual $CHCl_3$ was used as the internal reference δ = 7.26 ppm. A solution of the host **1** or **2** was prepared in 500 μl $CDCl_3$ (0.013 M) in a clean, dry NMR tube. The guest **3** stock solution was similarly prepared in 1.5 ml $CDCl_3$ (0.023 M) and titrated into the NMR tube *via* Hamilton microlitre syringe. Except for the first data point, the concentrations were calculated using the integration of tetramethylsilane as an internal standard. The ^{1}H-NMR spectra were recorded using a Bruker DPX400 spectrometer. The aromatic and N-H signals were monitored as successive aliquots of guest stock solution were added (15 additions up to 1500 μl).

The NMR titration data was analysed by numerical methods in a Microsoft Excel® spreadsheet using the standard 'Solver' feature. The spreadsheets are made available at http://go.warwick.ac.uk/marshgroup. The NMRTit program was kindly provided by Professor C. A. Hunter, University of Sheffield, implemented on an Apple Macintosh 7200/90 and the graphical data captured as a screenshot. A detailed description of the curve-fitting method along with the ITC experiment is provided in the Supporting Information.

Computational experiments:

Calculations were carried out on a PC workstation using MOE 2006.08 and the MMFF94x force field as supplied. Solvation effects were treated *via* the reaction field electrostatic term with a solvent dielectric of 10. Dihedral restraints were applied using both *ortho* carbons adjacent to the alkyne bond(s) such that a torsion angle of zero

corresponded to *syn* NH_2 groups. Stepped rotations around the alkyne bond(s) were achieved by applying torsional restraints in 15 degree increments for four complete rotations to generate the energy profiles in **Figures 15** and **16**. Any restraint energy was subtracted from the total and the dihedral angle used in the plots corresponds to the average of the actual dihedrals. Two restraints were essential to prevent non-colinearity of the alkyne bonds, particularly for receptor **2**.

Acknowledgments. AL would like to thank the Department of Chemistry, University of Warwick for funding. The authors also thank the reviewers for very useful comments and suggestions and Dr David Fox, University of Warwick, Department of Chemistry for helpful discussions.

References.

1. J. D. Badjic, A. Nelson, S. J. Cantrill, W. B. Turnbull and J. F. Stoddart, *Acc. Chem. Res.*, 2005, **38**, 723-732.
2. G. Ercolani, *J. Phys. Chem. B*, 2003, **107**, 5052-5057.
3. A. Marquis, J. P. Kintzinger, R. Graff, P. N. W. Baxter and J. M. Lehn, *Angew. Chem. Intl. Edn.*, 2002, **41**, 2760-2764.
4. W. P. Jencks, *P. Natl. Acad. Sci. USA,* 1981, **78**, 4046-4050.
5. M. I. Page and W. P. Jencks, *P. Natl. Acad. Sci. USA*, 1971, **68**, 1678-&.
6. G. Ercolani, *J. Am. Chem. Soc.*, 2003, **125**, 16097-16103.
7. G. Ercolani, *Org. Lett.*, 2005, **7**, 803-805.
8. A. D. Hughes and E. V. Anslyn, *P. Natl. Acad. Sci. USA*, 2007, **104**, 6538-6543.
9. G. Ercolani, C. Piguet, M. Borkovec and J. Hamacek, *J. Phys. Chem. B*, 2007, **111**, 12195-12203.
10. J. L. Sessler, C. M. Lawrence and J. Jayawickramarajah, *Chem. Soc. Rev.*, 2007, **36**, 314-325.
11. A. Marsh, N. W. Alcock, W. Errington and R. Sagar, *Tetrahedron*, 2003, **59**, 5595-5601.
12. S. Stoncius, E. Orentas, E. Butkus, L. Ohrstrom, O. F. Wendt and K. Wärnmark, *J. Am. Chem. Soc.*, 2006, **128**, 8272-8285.
13. F. G. J. Odille, S. Jónsson, S. Stjernqvist, T. Rydén and K. Wärnmark, *Chem. Eur. J.*, 2007, **13**, 9617-9636.

14. K. A. Connors, *Binding Constants. The Measurement of Molecular Complex Stability.*, Wiley, Chichester, 1987.
15. L. Fielding, *Tetrahedron*, 2000, **56**, 6151-6170.
16. K. Hirose, *J. Incl. Phenom. Macrocycl. Chem.*, 2001, **39**, 193-209.
17. C. S. Wilcox, in *Frontiers in Supramolecular Organic Chemistry and Photochemistry*, eds. H.-J. Schneider, H. Durr and J.-M. Lehn, VCH, Editon edn., 1991.
18. H.-J. Schneider and A. K. Yatsimirsky, *Principles and Methods in Supramolecular Chemistry*, 1st edn., Wiley, 2000.
19. M. Saunders and J. B. Hyne, *J. Chem. Phys.*, 1958, **29**, 1319-1323.
20. S. C. Zimmerman and B. F. Duerr, *J. Org. Chem.*, 1992, **57**, 2215-2217.
21. SpecFit, http://www.bio-logic.info/rapid-kinetics/software.html, Accessed 7 November, 2008.
22. C. Frassineti, S. Ghelli, P. Gans, A. Sabatini, M. S. Moruzzi and A. Vacca, *Anal Biochem*, 1995, **231**, 374-382.
23. P. Kuzmic, *Anal. Biochem.*, 1996, **237**, 260-273.
24. Prism, http://www.graphpad.com/prism/prism.htm, Accessed 7 November, 2008.
25. M. J. Hynes, *J Chem Soc Dalton*, 1993, 311-312.
26. C. Frassineti, L. Alderighi, P. Gans, A. Sabatini, A. Vacca and S. Ghelli, *Anal. Bioanal. Chem.*, 2003, **376**, 1041-1052.
27. A. P. Bisson, C. A. Hunter, J. C. Morales and K. Young, *Chem. Eur. J.*, 1998, **4**, 845-851.
28. M. D. Cowart, I. Sucholeiki, R. R. Bukownik and C. S. Wilcox, *J. Am. Chem. Soc.*, 1988, **110**, 6204-6210.
29. V. G. H. Lafitte, A. E. Aliev, P. N. Horton, M. B. Hursthouse and H. C. Hailes, *Chem. Commun.*, 2006, 2173-2175.
30. J. P. Clare, A. J. Ayling, J. B. Joos, A. L. Sisson, G. Magro, M. N. Perez-Payan, T. N. Lambert, R. Shukla, B. D. Smith and A. P. Davis, *J. Am. Chem. Soc.*, 2005, **127**, 10739-10746.
31. H. Dodziuk, K. S. Nowinski, W. Kozminski and G. Dolgonos, *Org. Biomol. Chem.*, 2003, **1**, 581-584.
32. G. Pistolis and A. Malliaris, *Chem. Phys. Lett.*, 1999, **310**, 501-507.
33. G. Pistolis and A. Malliaris, *Chem. Phys. Lett.*, 1999, **303**, 334-340.
34. L. D. Williams, N. G. Williams and B. R. Shaw, *J. Am. Chem. Soc.*, 1990, **112**, 829-833.
35. J. Sartorius and H. J. Schneider, *Chem. Eur. J.*, 1996, **2**, 1446-1452.
36. D. C. Harris, *J. Chem. Educ.*, 1998, **75**, 119-121.
37. S. Walsh and D. Diamond, *Talanta*, 1995, **42**, 561-572.
38. R. B. Martin, *Chem. Rev.*, 1996, **96**, 3043-3064.
39. Y. Cohen, L. Avram and L. Frish, *Angew. Chem. Intl. Edn.*, 2005, **44**, 520-554.
40. K. A. Dill and S. Bromberg, *Molecular Driving Forces: statistical thermodynamics in chemistry and biology*, Garland Science, New York, 2003.
41. L. D. Williams, B. Chawla and B. R. Shaw, *Biopolymers*, 1987, **26**, 591-603.
42. G. Gottarelli, S. Masiero, E. Mezzina, G. P. Spada, P. Mariani and M. Recanatini, *Helv. Chim. Acta,*, 1998, **81**, 2078-2092.

43. G. Gottarelli, S. Masiero, E. Mezzina, S. Pieraccini, J. P. Rabe, P. Samori and G. P. Spada, *Chem. Eur. J*, 2000, **6**, 3242-3248.
44. T. Giorgi, F. Grepioni, I. Manet, P. Mariani, S. Masiero, E. Mezzina, S. Pieraccini, L. Saturni, G. P. Spada and G. Gottarelli, *Chem. Eur. J*, 2002, **8**, 2143-2152.
45. M. C. Masiker, C. L. Mayne and E. M. Eyring, *Magn. Reson. Chem.*, 2006, **44**, 220-229.
46. C. Nativi, M. Cacciarini, O. Francesconi, A. Vacca, G. Moneti, A. Ienco and S. Roelens, *J Am Chem Soc*, 2007, **129**, 4377-4385.
47. C. S. Wilcox, J. J. C. Adrian, T. H. Webb and F. J. Zawacki, *J. Am. Chem. Soc.*, 1992, **114**, 10189-10197.
48. A. Vacca, C. Nativi, M. Cacciarini, R. Pergoli and S. Roelens, *J. Am. Chem. Soc.*, 2004, **126**, 16456-16465.
49. S. C. Zimmerman, P. S. Corbin and B. Xie, *Struct. Bond.*, 2000, **96**, 63-94.
50. MOE2006.08, *Chemical Computing Group, Montreal, 2006.*
51. Z. Rodriguez-Docampo, S. I. Pascu, S. Kubik and S. Otto, *J. Am. Chem. Soc.*, 2006, **128**, 11206-11210.
52. S. Otto, *J. Chem. Soc., Dalton Trans.*, 2006, 2861-2864.
53. J. Hamacek and C. Piguet, *J. Phys. Chem. B*, 2006, **110**, 7783-7792.
54. A. Horovitz and A. R. Fersht, *J. Mol. Biol.*, 1990, **214**, 613-617.
55. J. Wyman and S. J. Gill, *Binding and linkage: functional chemistry of biological macromolecules*, University Science Books, Mill Valley, Calif., 1990.
56. E. Di Cera, *Thermodynamic theory of site-specific binding processes in biological macromolecules*, Cambridge University Press, Cambridge, 1995.

Graphical Abstract

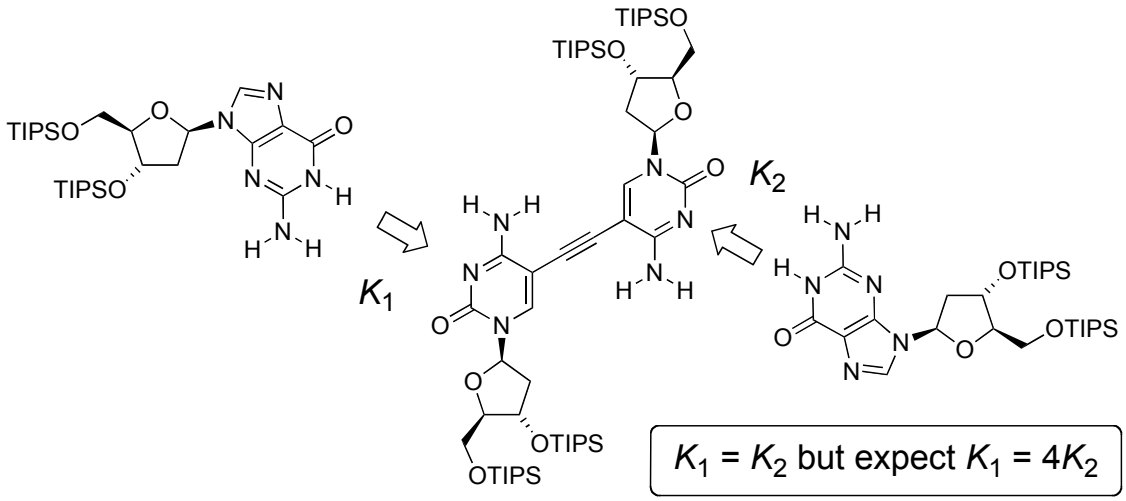

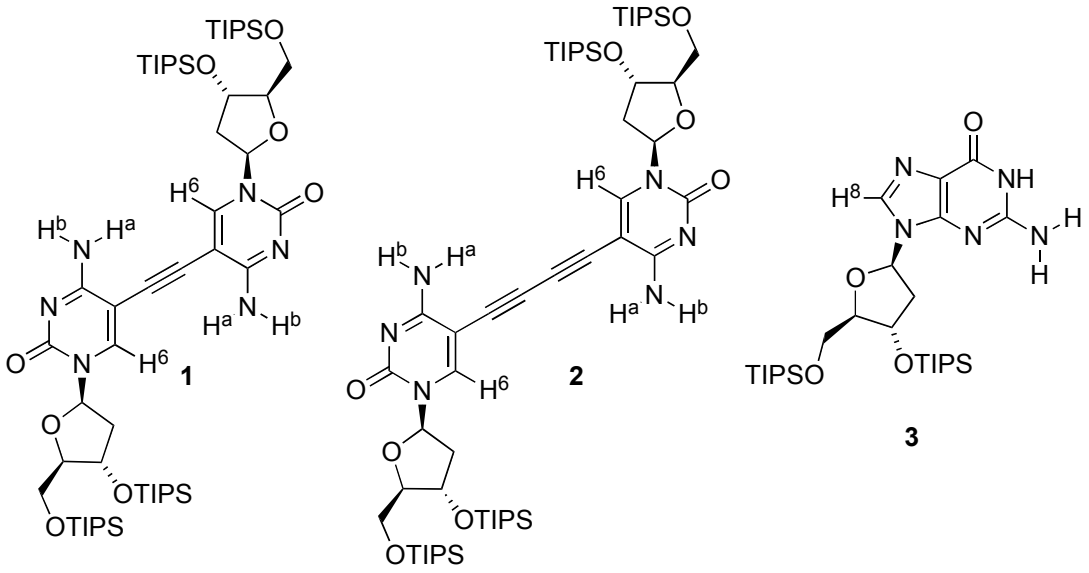

Figure 1. Receptors **1**, **2** and guanosine derivative, **3** used for binding studies; TIPS = triisopropylsilyl.

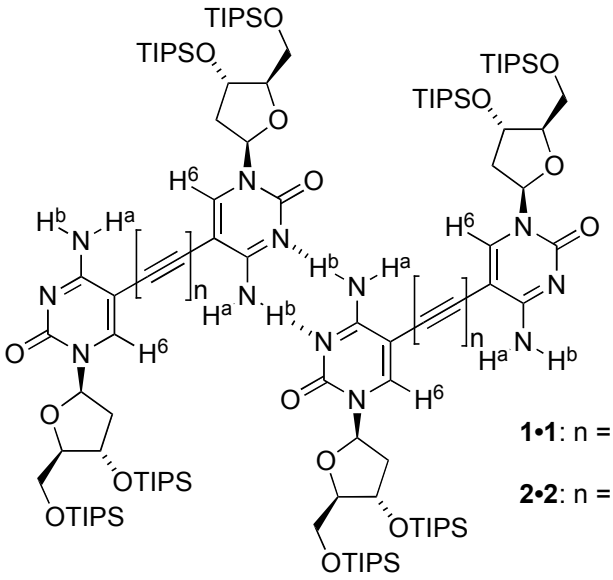

Figure 2. Dimers of **1** and **2, 1•1** and **2•2**; respectively.

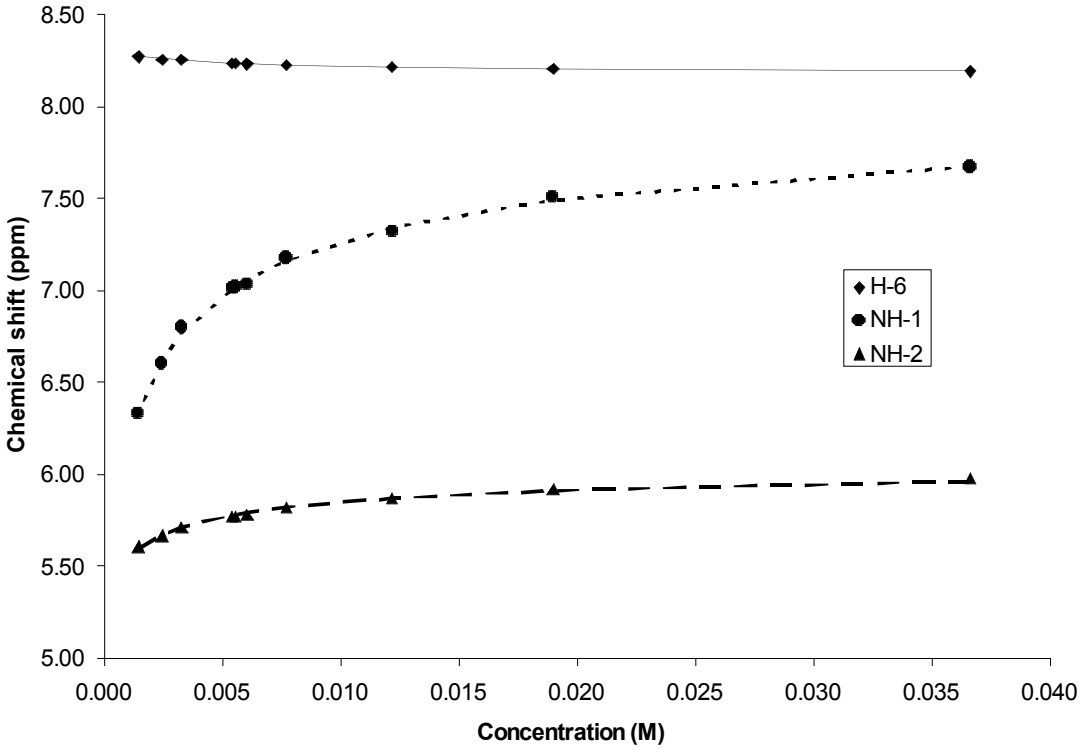

Figure 3. Curve fitting from NMR dilution of **2**; $K_{\mathbf{2}\cdot\mathbf{2}} = 340\pm7\ M^{-1}$.

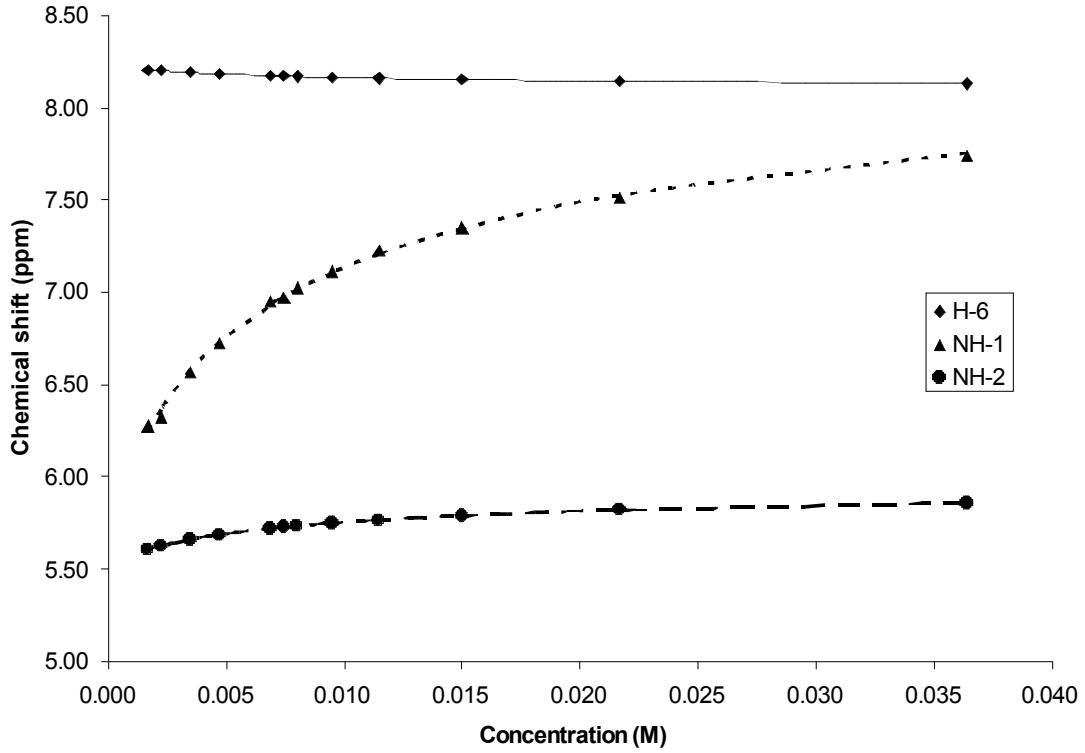

Figure 4. Curve fitting from NMR dilution of **1** in $CDCl_3$; $K_{\mathbf{1}\cdot\mathbf{1}} = 83\pm3\ M^{-1}$.

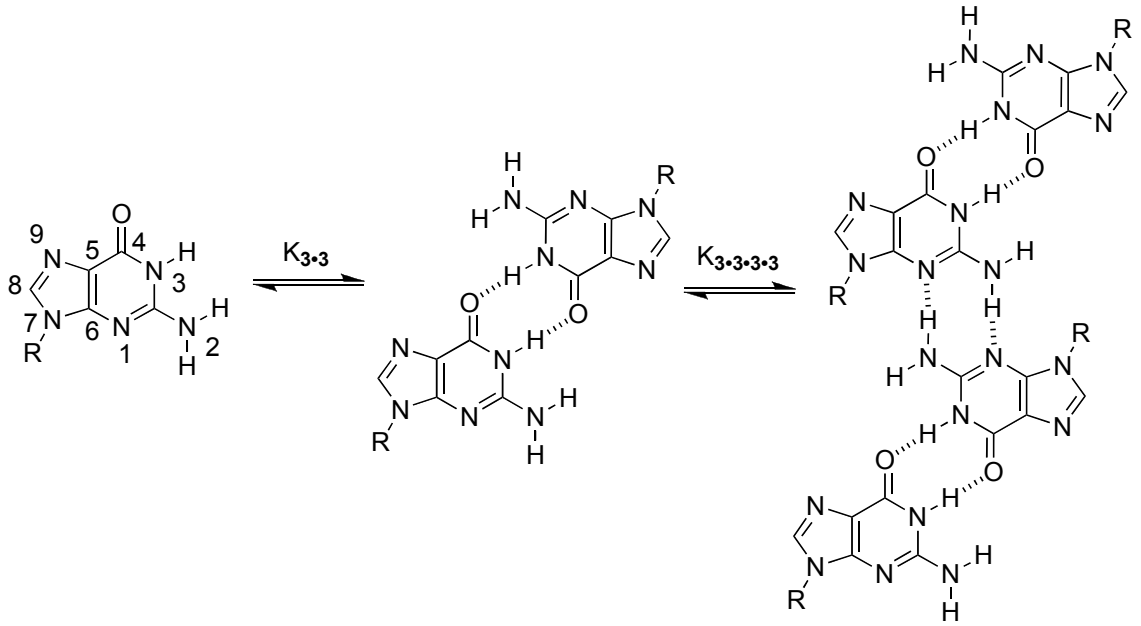

Figure 5. Self-association model of lipophilic guanosine **3** in chloroform.

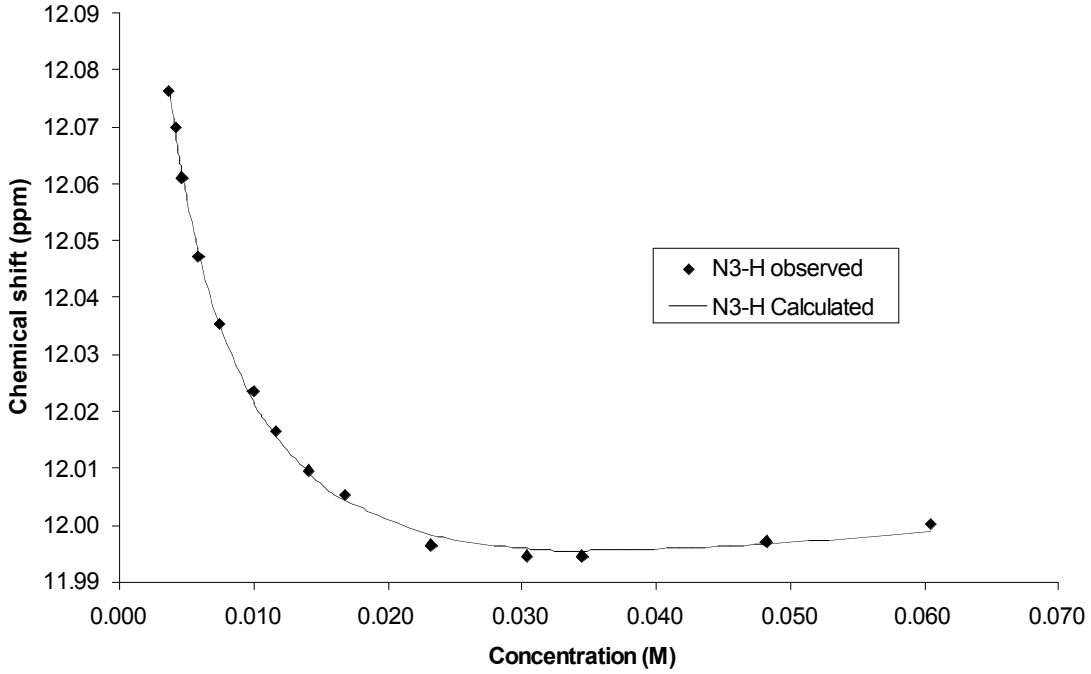
12.09
12.08
12.07
12.06
12.05
12.04
12.03
12.02
12.01
12.00
11.99
Chemical shift (ppm)
0.000
0.010
0.020
0.030
0.040
0.050
0.060
0.070
Concentration (M)
N3-H observed
N3-H Calculated

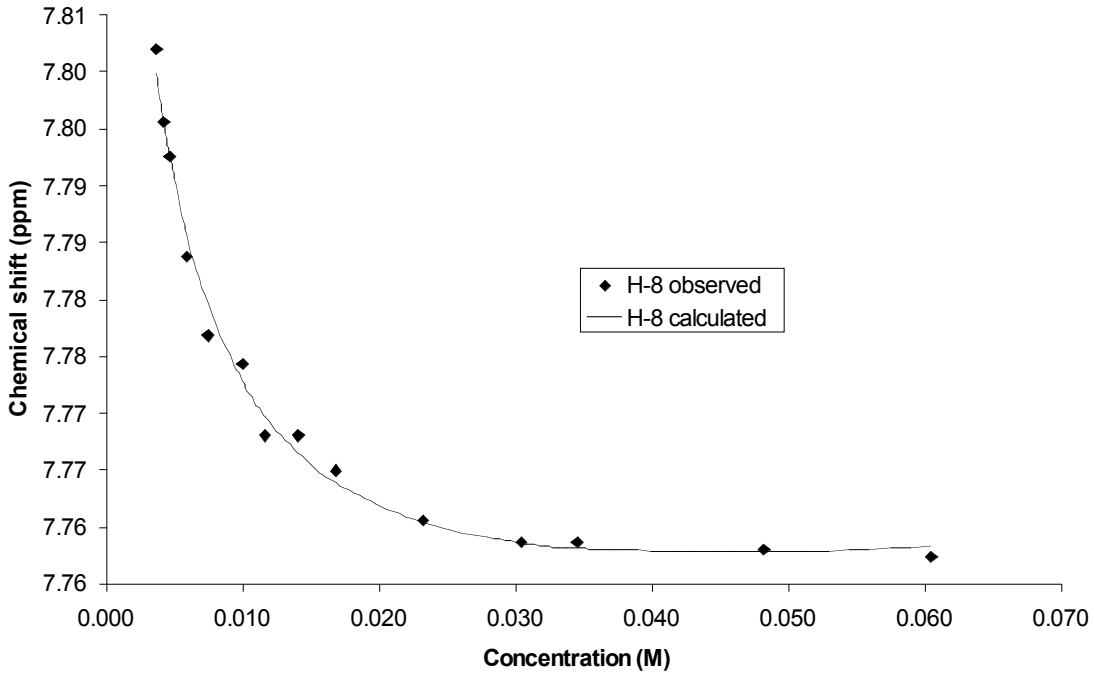
7.81
7.80
7.80
7.79
7.79
7.78
7.78
7.77
7.77
7.76
7.76
Chemical shift (ppm)
0.000
0.010
0.020
0.030
0.040
0.050
0.060
0.070
Concentration (M)
H-8 observed
H-8 calculated

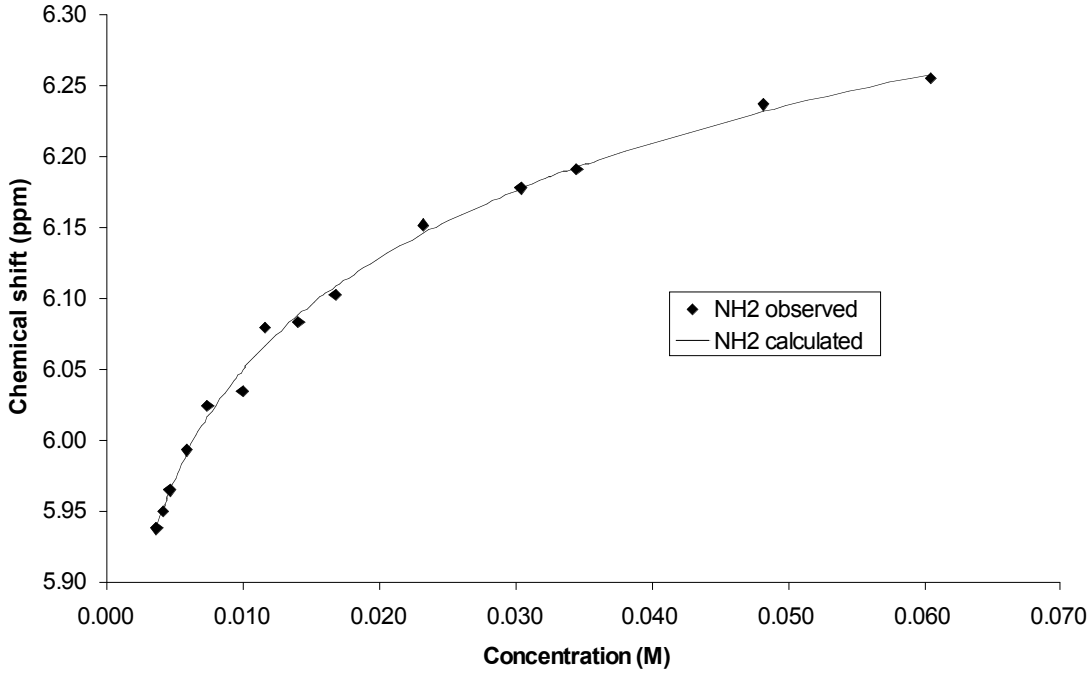

Figure 6. Curve fitting for NMR dilution of **3** in $CDCl_3$. The three titration curves (**A**) N3-H (**B**) H-8 and (**C**) NH_2 are fitted simultaneously to give $K_{\mathbf{3}\cdot\mathbf{3}}$ of 370±72 and $K_{\mathbf{3}\cdot\mathbf{3}\cdot\mathbf{3}\cdot\mathbf{3}}$ of 15±1 M^{-1}.

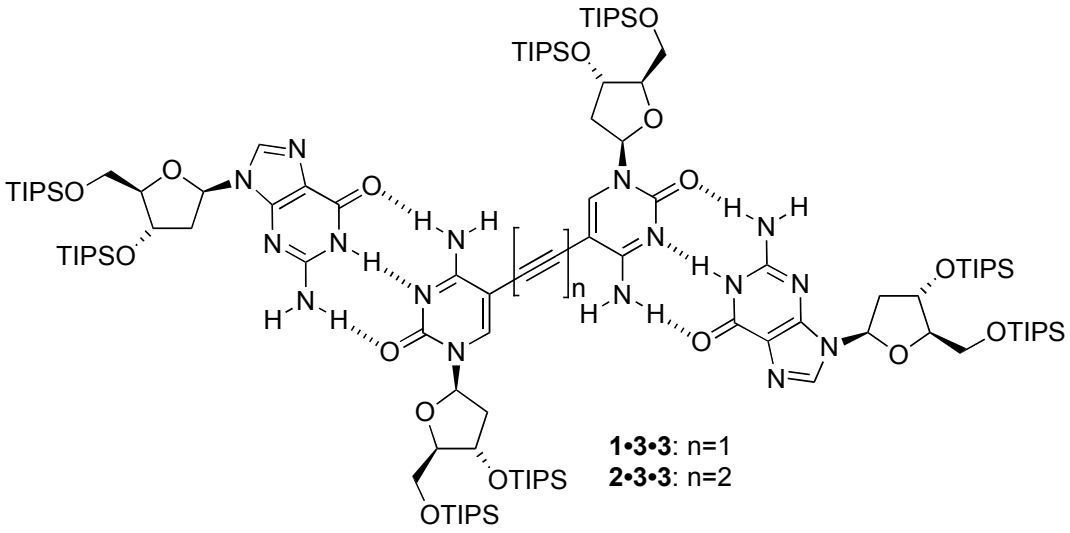

Figure 7. Complexation of receptors **1** or **2** with **3**; TIPS = triisopropylsilyl.

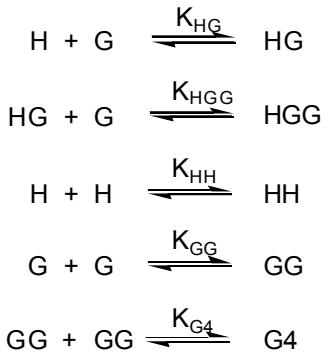

Scheme 1. Equilibria in the binding studies between **2** and **3**.

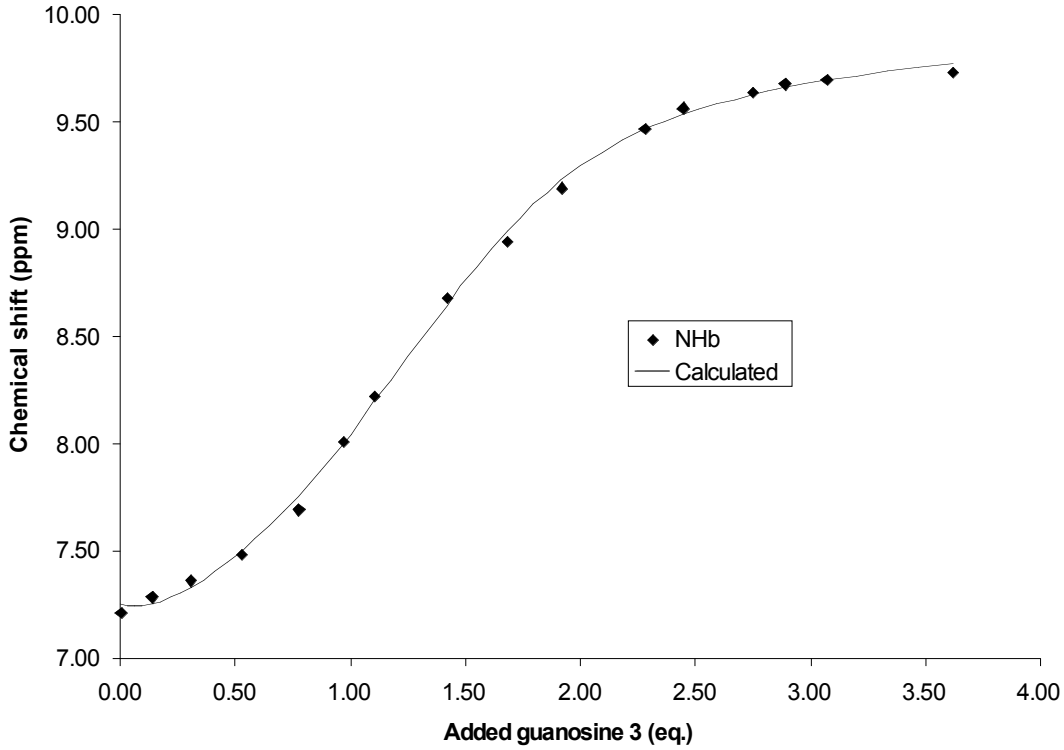

Figure 8. Curve fitting of NMR titration in $CDCl_3$ between **2** and **3**. $K_{\mathbf{2}\bullet\mathbf{3}}$ 8100 ± 380; $K_{\mathbf{2}\bullet\mathbf{3}\bullet\mathbf{3}}$ 1170 ± 80 M^{-1}.

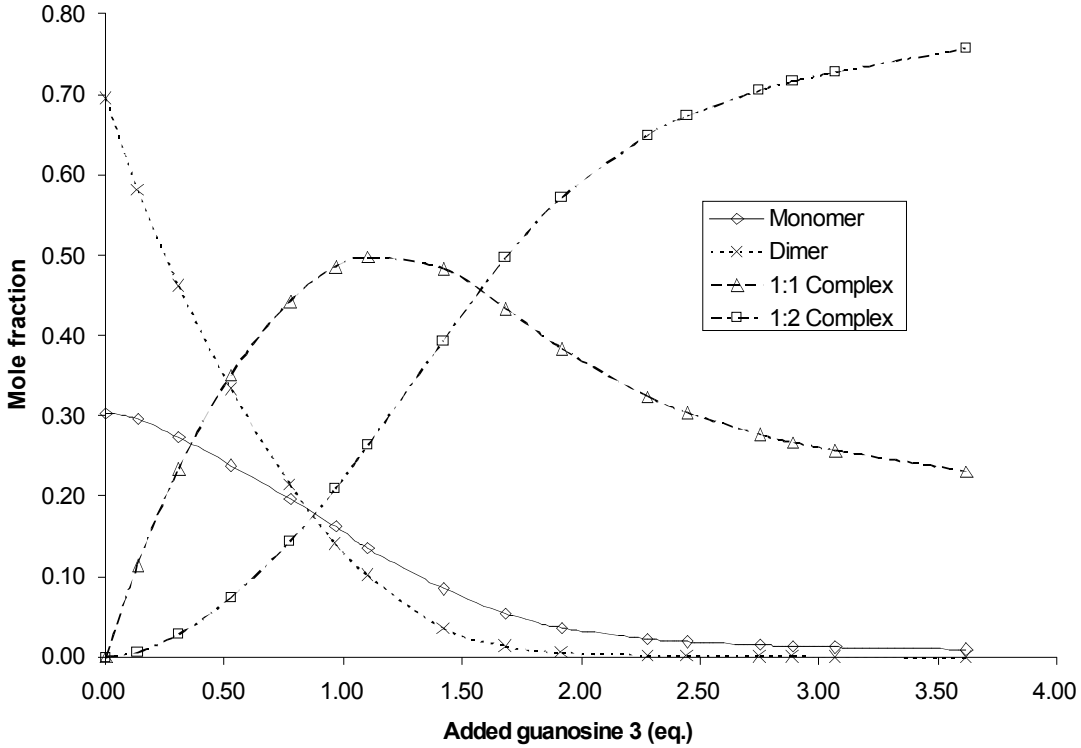

Figure 9. Speciation curve for receptor **2** upon addition of **3** in $CDCl_3$, showing monomeric **2**, dimeric **2,** 1:1 complex (**2•3**) and 1:2 complex (**2•3•3**).

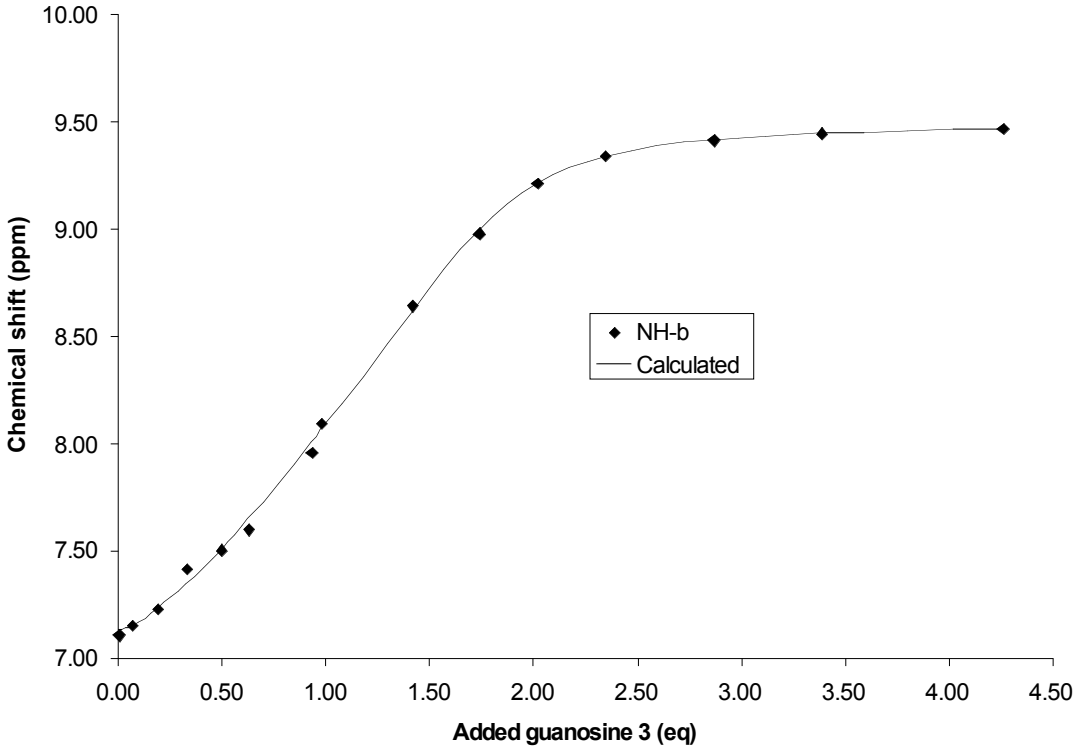

Figure 10. Curve fitting of NMR titration in $CDCl_3$ between **1** and **3**. $K_{\mathbf{1}\cdot\mathbf{3}} = 5180 \pm 210$, $K_{\mathbf{1}\cdot\mathbf{3}\cdot\mathbf{3}} = 4800 \pm 170\ M^{-1}$.

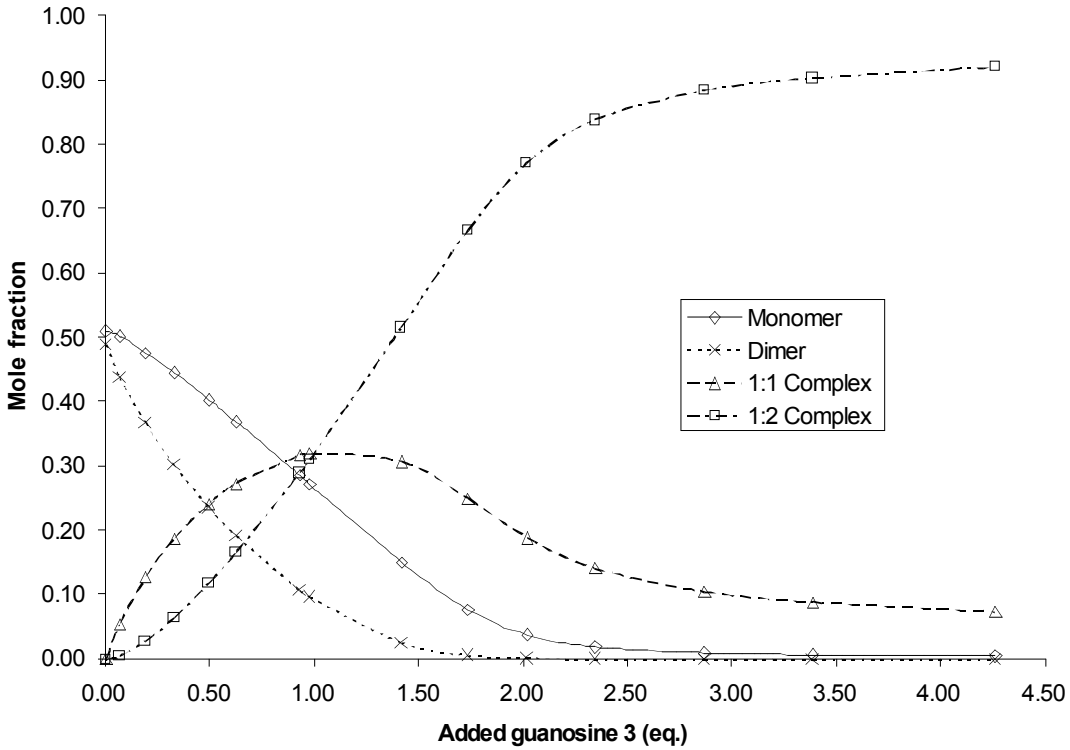

Figure 11. Speciation curve for **1** upon addition of **3** in $CDCl_3$.

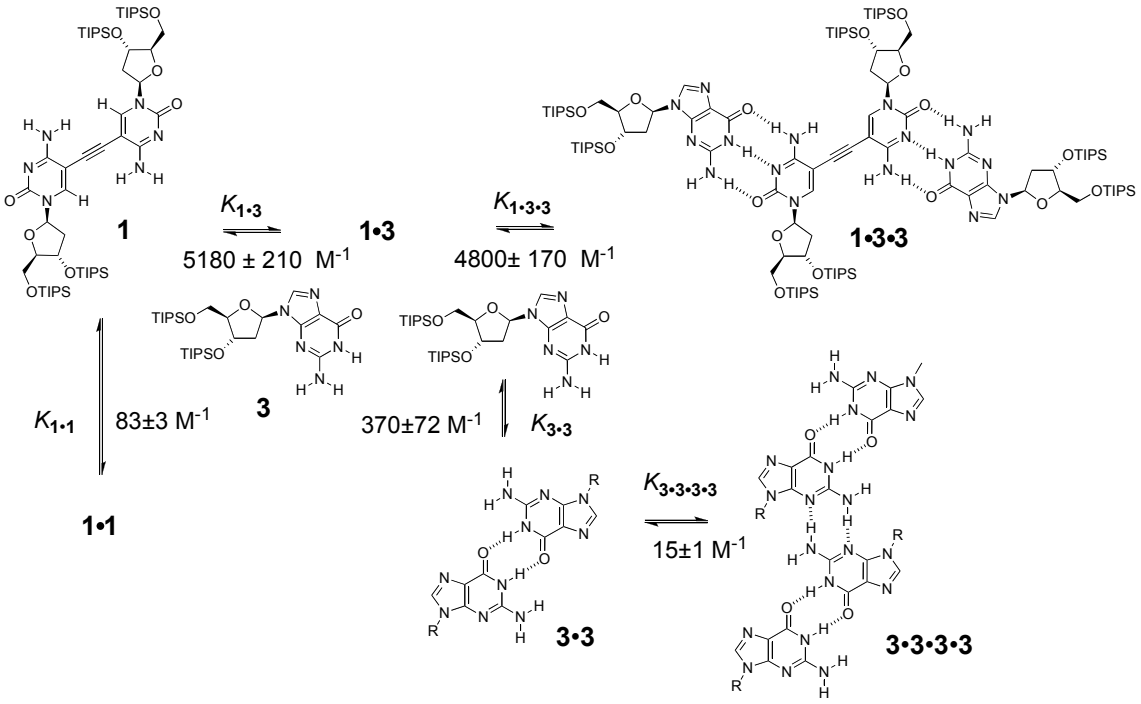

Figure 12. Summary of equilibria in deuterochloroform for monoalkyne receptor **1.**

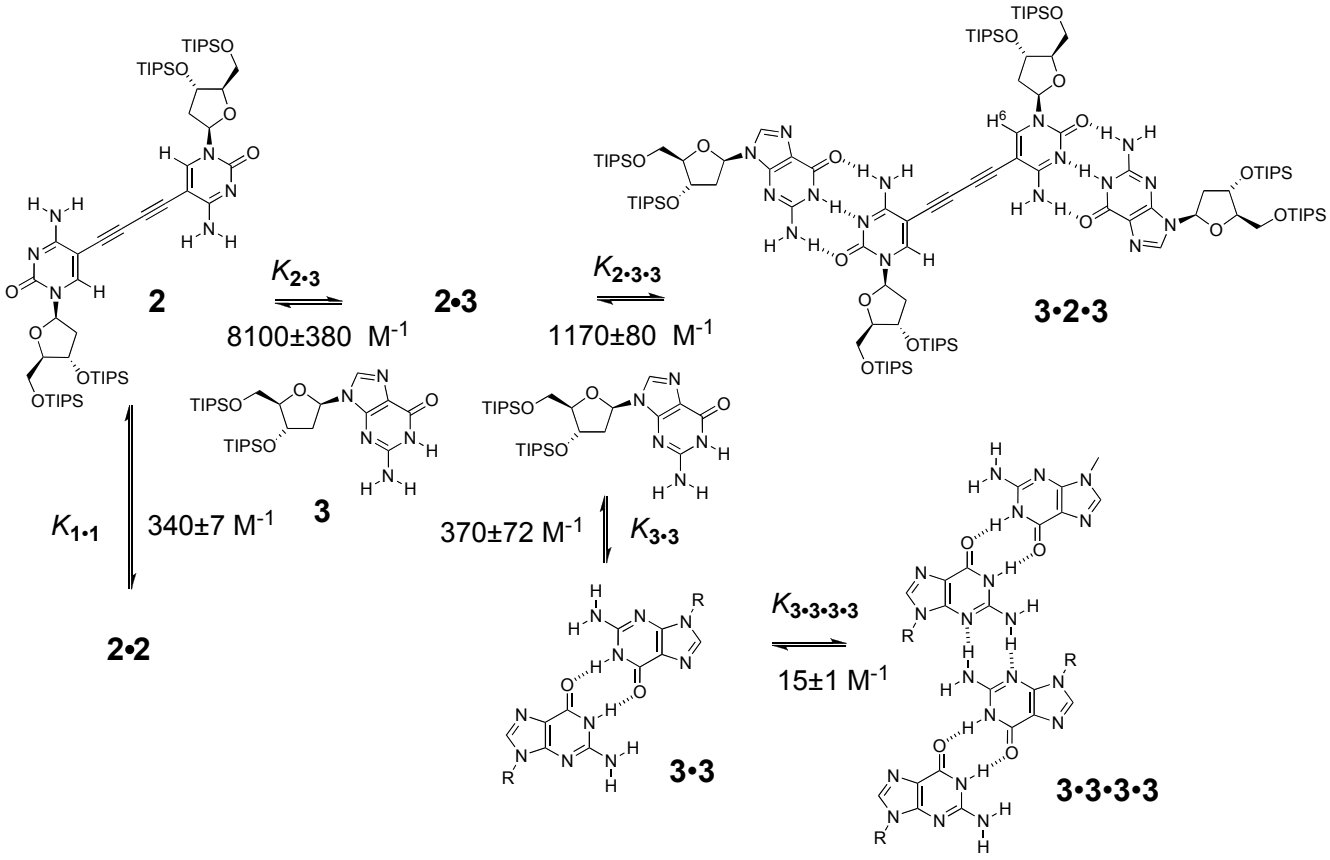

Figure 13. Summary of equilibria in deuterochloroform for dialkyne receptor **2**.

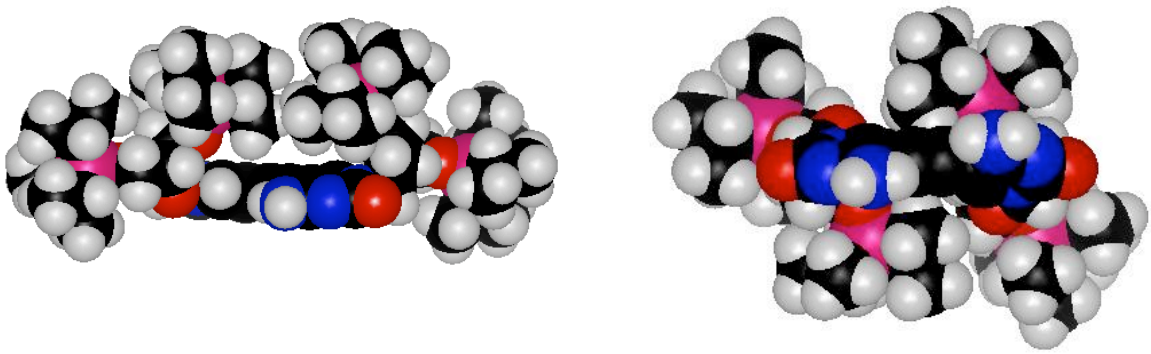

Figure 14. C-P-K models of **1** at E_{min}(left) dihedral ≈ 30° showing interactions between TIPS groups and E_{max} (right) dihedral ≈ 165°.

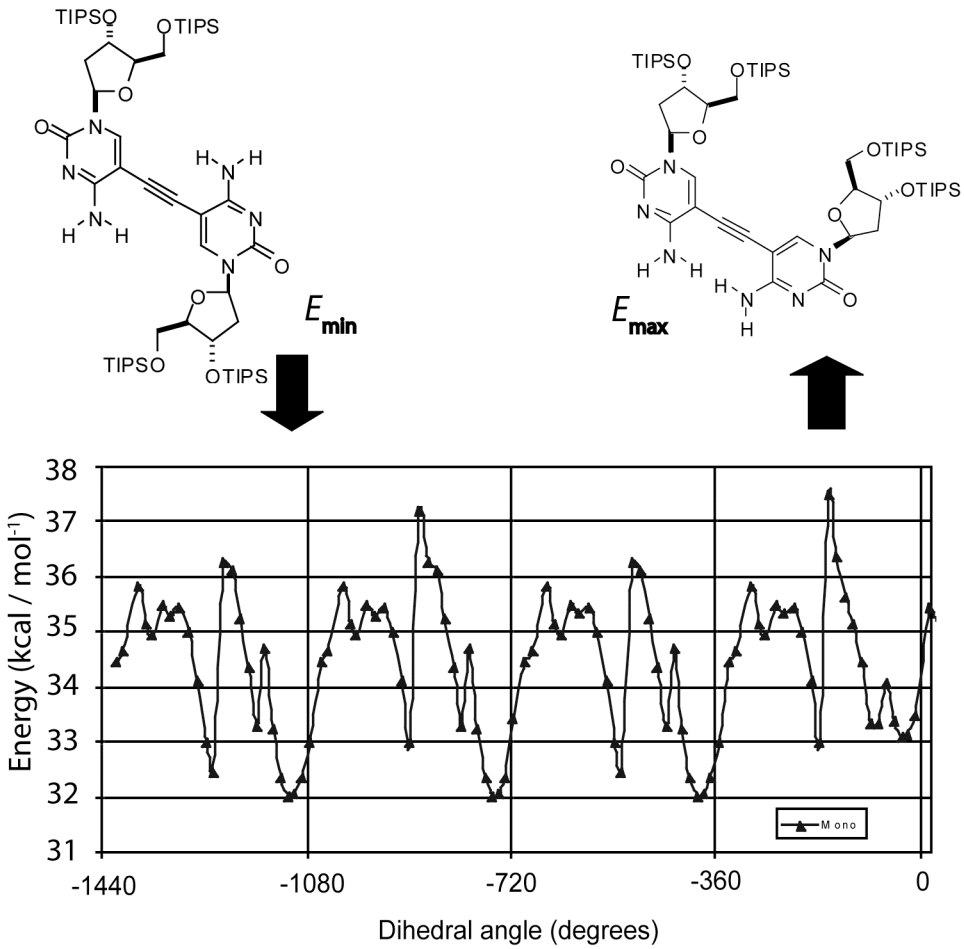

Figure 15. Torsional energy *vs*. dihedral angle for monoalkyne **1**

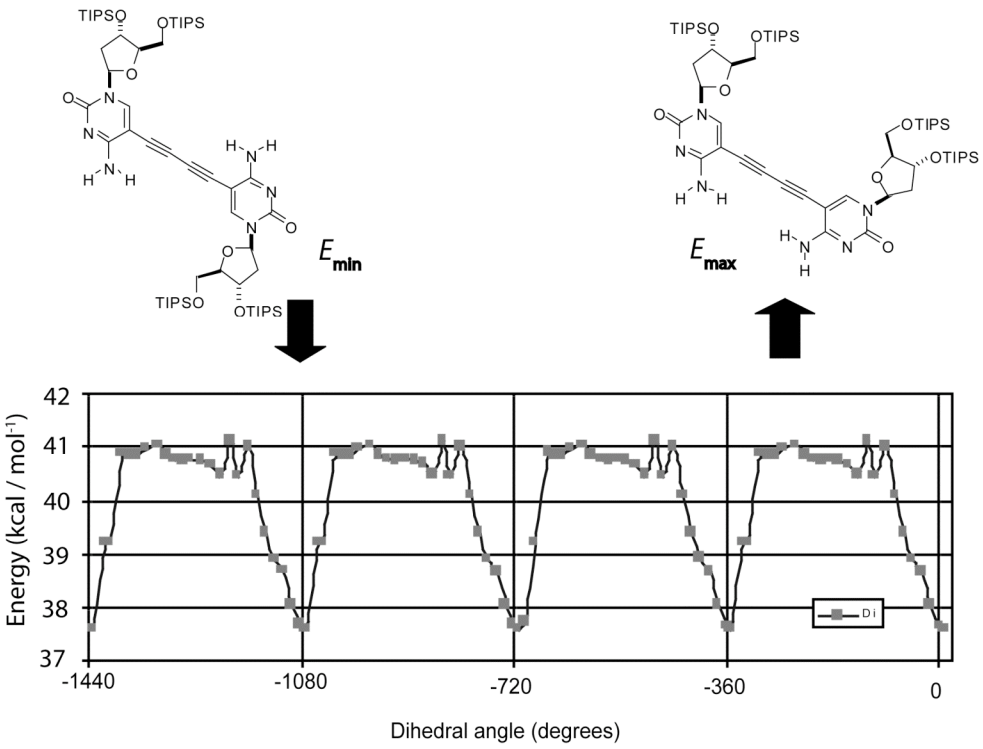

Figure 16. Torsional energy *vs*. dihedral angle for dialkyne **2**